Microporous and Mesoporous Materials 317 (2021) 110946

Contents lists available at ScienceDirect

Microporous and Mesoporous Materials

journal homepage: http://www.elsevier.com/locate/micromeso

Synthesis of amorphous magnesium silicates with different SiO_2:MgO molar ratios at laboratory and pilot plant scales

Yolanda Aysa-Martínez [a,b], Silvia Anoro-López [c], Miguel Cano [c,**], Daniel Julve [c], Jorge Pérez [c], Joaquín Coronas [a,b,*]

[a] Instituto de Nanociencia y Materiales de Aragón (INMA), Universidad de Zaragoza-CSIC, 50018, Zaragoza, Spain
[b] Chemical and Environmental Engineering Department, Universidad de Zaragoza, 50018, Zaragoza, Spain
[c] Industrias Químicas del Ebro S. A. Grupo IQE. 50016, Zaragoza, Spain

ARTICLE INFO

Keywords:
Amorphous magnesium silicate
Magnesium sulfate
Sodium silicate
Precipitation process
Scale-up

ABSTRACT

In this study, amorphous magnesium silicates with different SiO_2:MgO molar ratios were synthesized by a precipitation reaction from magnesium sulfate ($MgSO_4$), sodium silicate (Na_2SiO_3) and water. At laboratory scale, it was studied the effect of the SiO_2:Na_2O molar ratio of the Na_2SiO_3 solution used as a reagent on the properties of the amorphous magnesium silicates obtained. It was observed that this ratio is a key parameter in the synthesis process of these materials. The chemical composition and principal physicochemical properties were established, including textural properties from nitrogen adsorption/desorption isotherms and X-ray fluorescence. Moreover, some laboratory tests were scaled-up in an industrial pilot plant (ca. 10^3 times larger, i.e. 700 kg of wet product) demonstrating the high scalability of the materials obtained. The properties of the scaled-up materials were compared to those of different commercial materials containing magnesium silicate, such as Florisil® and Magnesia 430®. Analogous properties were achieved in terms of particle size distribution, humidity and pH and conductivity in solution.

1. Introduction

Magnesium silicates exist naturally and synthetically. They can be classified into three large groups: dense hydrated magnesium silicates (DHMS), magnesium phyllosilicates and amorphous magnesium silicates. DHMS includes the so-called "alphabetic phases", these being phases A, B, C [1], D [2], E, F [3], G [4] and superhydrous phase B [5]. Due to the fact that all of them exist naturally in the mantle and in the subduction zones of the Earth, their syntheses require conditions of high pressure and temperature [6]. Magnesium phyllosilicates, such as talc or sepiolite, are crystalline and can be found in the Earth's crust; they can be obtained under moderate hydrothermal conditions [7]. Amorphous magnesium silicates are synthetic and can be produced by sol-gel method [8], precipitation [9,10] or by a mechano-chemical process [11].

The most common route for the synthesis of amorphous magnesium silicates is by a precipitation reaction between a soluble silicate, mainly sodium silicate (Na_2SiO_3, generally represented by the formula $r \cdot SiO_2 \cdot Na_2O$ [9], where "r" is the SiO_2:Na_2O molar ratio) and a soluble magnesium salt, such as magnesium sulfate ($MgSO_4$) [12], magnesium nitrate ($Mg(NO_3)_2$) [13] or magnesium chloride ($MgCl_2$) [14].

The formation of amorphous magnesium silicate consists of individual stages that occur simultaneously. These are: the formation of silicic acid (H_4SiO_4, whose source is the soluble silicate used as raw material) and its subsequent polymerization to form nuclei that react with the magnesium salt thus constituting the final magnesium silicate product.

The surface of amorphous magnesium silicate is composed of siloxane groups (Si–O–Si), silanol groups (Si–OH), silanolan groups (Si–O–Na) and magnesil groups (Si–O–Mg–OH). The most reactive groups on the surface are free hydroxyl groups (silanol groups). These are responsible for providing the sites for the physical adsorption of organic molecules and easily react with multiple substituents [15,16], justifying the practical interest of magnesium silicate. In addition, being silanols replaced by new compounds, they provide potential for surface modification.

* Corresponding author. Instituto de Nanociencia y Materiales de Aragón (INMA), Universidad de Zaragoza-CSIC, 50018, Zaragoza, Spain.
** Corresponding author.
E-mail addresses: mcano@iqe.es (M. Cano), coronas@unizar.es (J. Coronas).

https://doi.org/10.1016/j.micromeso.2021.110946
Received 21 October 2020; Received in revised form 20 January 2021; Accepted 29 January 2021
Available online 23 February 2021

Table 1
Reagents used in the precipitation of amorphous magnesium silicates.

Reagent	State	Concentration	Supplier
Sodium silicate	aqueous solution	r (SiO_2:Na_2O in weight) ~ 2 and 3.35	IQE, S.A.
Magnesium sulfate	solid	100% $MgSO_4 \cdot 7H_2O$	Magnesia GmbH
Brine	aqueous solution	NaCl ≥ 285 g/L	IQE, S.A.
Deionized water	liquid	-	Productos Gilca, S.C.

Amorphous magnesium silicate is widely used in the pharmaceutical and food industries as well as in other industrial fields such as rubber, paper or paintings, and it also has application in chromatography. Amorphous magnesium silicate can be used as a glidant and anti-caking agent in oral formulations in the pharmaceutical industry and in food products [17]. Besides, this compound is used as a carrier for fragrances and flavors in the food industry [18]. Moreover, its white color can easily compete with titanate-based pigments, which would eliminate, partially or totally, the use of titanium dioxide in certain foods and paint formulations [9]. Finally, amorphous magnesium silicate is used as a filler for many silicone and rubber products [19], as a filler and pigment in dispersive paintings, as an adsorbent in chromatography [9] and as a filler in papermaking to improve its printing capacity and opacity [20].

This study focuses on the synthesis of amorphous magnesium silicates from magnesium sulfate, sodium silicate and water both at laboratory and industrial pilot plant scales. The effect of reaction composition on the textural properties and chemical composition of the silicates was studied demonstrating the scalability of the materials obtained comparable to analogous commercial products.

2. Experimental section

2.1. Materials

The raw materials used in this work, listed in Table 1, are: sodium silicate (Na_2SiO_3), magnesium sulfate ($MgSO_4$), brine (NaCl solution) and deionized water. Due to the fact that the dosage of the reagents was carried out through peristaltic pumps, it was necessary to prepare the aqueous solution corresponding to $MgSO_4$ for each experiment. Thus, the necessary amount of $MgSO_4 \cdot 7H_2O$ for each experiment was weighted to prepare an aqueous solution in the 14–17 w% range of $MgSO_4 \cdot 7H_2O$ and it was stirred at room temperature until the complete dissolution of the salt.

2.2. Procedure

The synthesis procedures carried out in the experimental plant at laboratory scale and in the industrial pilot plant followed the same steps, which were: preparation of the initial bed of precipitation, precipitation (reagent dosing), maturation, filtering, washing with water and drying. The proposed flowchart is shown in Fig. 1a.

Each production process was monitored through a control interface. In the case of laboratory scale, the precipitation zone had a touch interface based electronic system (Omron Co.) and in the industrial pilot plant the control was carried out through a supervisory control and data acquisition (SCADA) system.

In each reaction run, the following parameters were kept constant: reagent dosing time (2 h, corresponding to the precipitation time), maturation time (3 h), reaction temperature (70 °C), Na_2SiO_3 and brine concentration in the initial reactor bed (3.5 and 1 wt%, respectively, with respect to the total amount of deionized water present in the initial bed), water concentration in the reactor bed (twice that of the total Na_2SiO_3 required for the reaction process) and dry matter concentration in the reaction bed (6 wt%). Furthermore, the moles of SiO_2 at laboratory scale were in the range of 0.6–0.7 and in the industrial pilot plant were approximately 10^3 larger.

2.2.1. Initial bed preparation

Before beginning the precipitation, the precipitation bed must be prepared. To do this, deionized water and brine were introduced into the reactor. Subsequently, the solution was heated to 70 °C at the same time as the stirring begins. Once the working temperature was reached, the amount of Na_2SiO_3 belonging to the initial bed was added.

The Na_2SiO_3 that was part of the initial bed of the reactor aimed at controlling the initial pH and, therefore, it eliminated the possible variation of the properties of the final product by this parameter. In addition, brine was added to maintain a high level of ionic strength to avoid a flocculation process of the particles.

2.2.2. Precipitation

Once the precipitation bed was prepared and the working temperature was reached, the dosing of the Na_2SiO_3 and $MgSO_4$ solutions to the

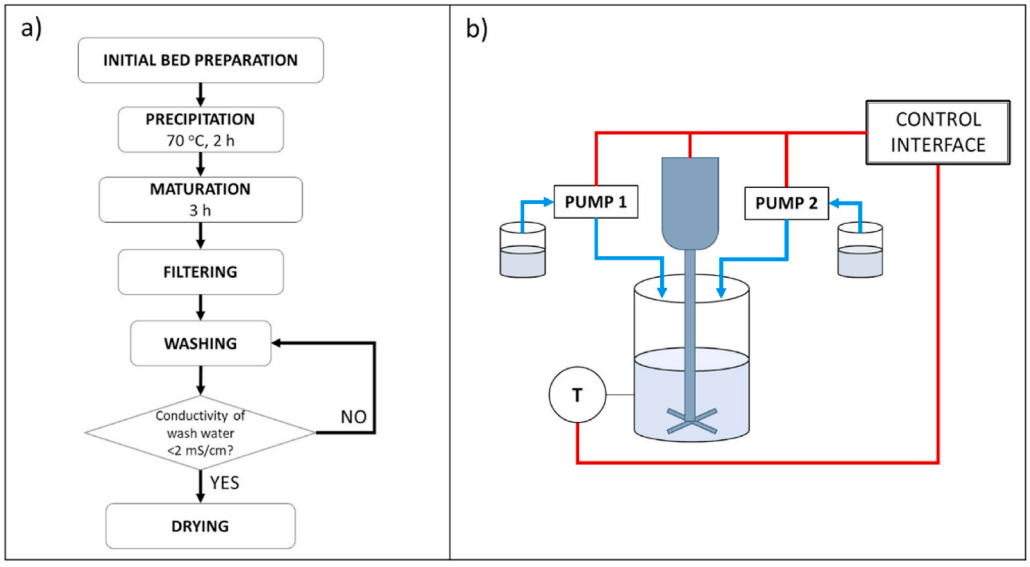

Fig. 1. a) Flowchart, and b) precipitation zone diagram of the amorphous magnesium silicate synthesis process.

reactor started. Dosing was carried out simultaneously for 2 h through the corresponding pumps. Fig. 1b depicts a diagram of the precipitation zone corresponding to the process of synsthesis of the amorphous magnesium silicates.

At laboratory scale, the dosage of the reagents to the reactor, which were stored in 250 mL Pyrex beakers, was carried out using two peristaltic pumps (D-25Vplus, Dinko Instruments). The reaction was conducted in a Pyrex tank of 2 L capacity. The reactor was placed in a magnetic stirrer (C-MAG HS 7, IKA) with its corresponding temperature probe (ETS-D5, IKA) for continuous temperature control and it was equipped with a top stirrer (Heidolph-TORQUE 400) which secured intense mixing of the system.

In the industrial pilot plant, the reaction area consists of two 700 L tanks in which the raw materials (Na_2SiO_3 and $MgSO_4$ solutions) were stored, and a 1350 L reactor. All these units have stirrers inside. The reactor has a temperature probe (PT 100, SEDEM) and an indirect heat supply system through steam. The reagents were fed to the reactor using membrane pumps (N–P31, Bran Luebbe).

As the reagents were dosed, the following chemical reaction (Equation (1)) occurred between them:

$$rSiO_2 \cdot Na_2O\ (aq) + MgSO_4(aq) \rightarrow rSiO_2 \cdot MgO\ (s) + Na_2SO_4(aq) \quad [1]$$

Sodium sulfate (Na_2SO_4) is formed as a by-product of the reaction. This substance is highly soluble in water. In consequence, it remained in solution in the reactor bed as it originated, and subsequently it was removed with the wash water.

2.2.3. Maturation

Once the reaction stage was finished, the temperature and stirring were maintained for 3 h so that the magnesium silicate produced continued to evolve. To track the product, samples were taken (at least 100 mL of wet product) at different maturation times (1 h and 3 h).

2.2.4. Filtration, washing and drying

After 3 h of maturation, the magnesium silicate obtained was separated from the reaction mixture by filtration and washed with deionized water to ensure that the Na_2SO_4 was eliminated. Finally, the resulting cake was subjected to a drying process as it contains a high amount of water that must be removed from the product.

At laboratory scale, the magnesium silicate was filtered and washed with deionized water at room temperature through a system made up of a Büchner funnel, a Bunsen flask and a vacuum pump (D-95, Dinko Instruments). Once the product was washed, the resulting cake was dried in an oven. Finally, the amorphous magnesium silicate particles obtained were subjected to a grinding process to obtain a more homogeneous product.

In the industrial pilot plant, the reactor content was pumped to a filter press, where the magnesium silicate was filtered and washed with deionized water at room temperature. Then, the wet cake obtained was fed to a spin-flash dryer to reduce the humidity of the product up to a certain level. The air inlet temperature in the drying chamber was above 200 °C, while the air outlet temperature was in the range of 120–150 °C. Due to agitation, collisions (with the walls and between particles) and drying caused by hot air, small and light particles were generated that leave the drying chamber at the top. These particles were collected by a series of cyclones and a bag filter.

2.3. Characterization techniques

In order to know the properties of the magnesium silicates synthesized, the characterization techniques presented below were used.

2.3.1. Characterization of magnesium silicates synthesized at laboratory scale

Through adsorption/desorption of nitrogen in the samples of the synthesized magnesium silicates, their specific surface areas were obtained by applying the BET method (Brunauer-Emmett-Teller). Each adsorption/desorption were carried out at 77 K by varying the relative pressure in a Micrometrics TRISTAR II PLUS equipment. Previously, the samples were degassed at 200 °C for 45 min, with a heating ramp of 10 °C/min.

Powder X-ray diffraction (XRD) was performed at room temperature in a D5000 S diffractometer with a copper anode and a graphite monochromator so as to select Cu−Kα_1 radiation ($\lambda = 1.5418$ Å). Measurements were carried out at 40 mA and 40 kV.

X-ray fluorescence (XRF) was applied as a method of semi-quantitative analysis of the oxides present in the final product of each experiment; that is, in the samples obtained at the end of the maturation stage once filtered, washed and dried. X-rays can penetrate a few micrometers into the powder sample what is enough due to the fact that the magnesium silicate powders here are constitute by primary nanometer particles. For this, a sequential XRF spectrophotometer from Thermo Electron ARL series was used. Due to the limitation of the technique some samples were selected to be analyzed.

Finally, it was possible to estimate the magnesium yield on the final product through Equation (2), where the numerator was obtained from the amount of magnesium present (estimated from the results of XRF) in the magnesium silicate produced, and the denominator was obtained knowing the amount of this compound present in the $MgSO_4$ solution prepared as a reactant.

$$\text{Mg yield } (\%) = \frac{\text{actual Mg amount in the final product obtained (g)}}{\text{Mg amount in MgSO4 reactant (g)}} \cdot 100 \quad [2]$$

2.3.2. Characterization of magnesium silicates synthesized in industrial pilot plant

In addition to the techniques used for the characterization of the products obtained at laboratory scale, the techniques presented below complete the characterization of magnesium silicates obtained in the industrial pilot plant.

Analysis of nitrogen adsorption and desorption isotherms obtained in stationary conditions allowed to estimate BET specific surface area, pore size distribution and pore volume applying the BJH method, and external surface area, micropore area and micropore volume through the t-plot method. Each adsorption/desorption isotherm was obtained at the same conditions as in the magnesium silicates obtained at laboratory scale and using the same equipment.

Wet laser diffraction (LD) was used as a method to determine the particle size distribution, as well as the average particle size (d_{50}). Measurements were performed using a Mastersizer 2000 laser diffraction instrument provided by Malvern Instruments. The instrument is powered by a Hydro 2000G dispersing unit supplied by Malvern Instruments.

The analysis of the moisture content of the samples was carried out through a moisture analyzer HB43–S from Mettler Toledo.

Through scanning electron microscopy (SEM), the morphology and particle size distribution of synthesized magnesium silicates were observed. The SEM images were obtained in a FEI-Inspect microscope. Transmission electron microscopy (TEM) images were taken using a FEI Tecnai T20, operated at 200 kV.

Finally, the conductivity and pH of the samples diluted at 5% (by weight) in deionized water at room temperature were measured. The equipment used for this test is a Thermo Scientific Orion Star A222 conductivity meter and a Crison GLP 21 pH-meter.

3. Results and discussion

3.1. Laboratory scale experiments

Na_2SiO_3 with a SiO_2:Na_2O molar ratio (r) of ca. 3.35 was used. Amorphous magnesium silicates were analyzed with different SiO_2:

Table 2
Properties of amorphous magnesium silicates. Laboratory scale experiments carried out at 70 °C and using a Na_2SiO_3 with a SiO_2:Na_2O molar ratio (r) of ca. 3.35.

Experiment	$R_{m,\ theoretical}$ (SiO_2:MgO)	Sample	Maturation time (h)	BET area (m^2/g)	$R_{m,\ actual}$ (SiO_2:MgO)	Mg Yield (%)
1	3.4	01	1	573	-	-
		02	3	599	3.8	88
2	2.7	01	1	583	-	-
		02	3	617	3.7	75
3	2.4	01	1	616	-	-
		02	3	639	3.9	70

Table 3
Properties of amorphous magnesium silicates. Laboratory scale experiments carried out at 70 °C and using a Na_2SiO_3 with a SiO_2:Na_2O molar ratio (r) of ca. 2.

Experiment	$R_{m,\ theoretical}$ (SiO_2:MgO)	Sample	Maturation time (h)	BET area (m^2/g)	$R_{m,\ actual}$ (SiO_2:MgO)	Mg Yield (%)
4	3.4	01	1	248	-	-
		02	3	242	2.8	100
5	2.4	01	1	616	-	-
		02	3	662	2.4	98

MgO molar ratios (R_m) by adjusting the molar flow ratio of the reagents.

Table 2 shows that all the obtained magnesium silicates, regardless of maturation time, have similar BET specific surface area values in the 573–639 m^2/g range. This suggests that 1 h maturation time is enough. Through XRF analysis, actual SiO_2:MgO molar ratios ($R_{m,\ actual}$) were obtained for some selected samples over the final products higher than the theoretical ones in each experiment ($R_{m,\ theoretical}$). This means that the product obtained did not contain all the MgO introduced as a reactant, and thus part of it remained in solution in the reaction bed as Mg^{2+} ions. Moreover, this fact is evidenced by the magnesium yields on the obtained products, since all the Mg yields in Table 2 are below 100%, in the 70–88% range. Similar values of $R_{m,\ actual}$ were found. That is, an equilibrium was reached between SiO_2 and MgO. The small differences between them can be attributed to the washing of the products, which can leave different amounts of Na_2O. The oxides present in the final products obtained by XRF are presented in Table S1.

Moreover, it is observed that, as expected, the magnesium yield improves when the $R_{m,\ theoretical}$ (i.e. the relative amount of Mg in the reaction medium) was higher. This is due to the fact that less magnesium was introduced into the precipitation reaction, because of that there was less magnesium in dissolution and, therefore, the magnesium yield on the final product increased.

3.1.1. *Effect of the SiO_2:Na_2O ratio of the Na_2SiO_3 used as a reactant*

To increase the magnesium yield in the final product, experiments using Na_2SiO_3 with a SiO_2:Na_2O ratio (r) of ca. 2 were carried out. The difference between this silicate and that of r ∼ 3.35 is the amount of Na_2O present in the solution. Na_2O expresses NaOH, so that when more NaOH is applied the degree of polymerization decreases, which means that SiO_2 units are in the form of either monomers or shorter polymers (oligomers) [21,22].

Two more experiments were carried out, one with $R_{m,\ theoretical} = 3.4$ and the other with $R_{m,\ theoretical} = 2.4$ (Table 3). Firstly, the experiments with a $R_{m,\ theoretical} = 3.4$ have BET specific surface areas around 250 m^2/g, while those with a $R_{m,\ theoretical} = 2.4$ show values around 600 m^2/g, both regardless of maturation time. Thus, the experiments with 1 and 3 h of maturation time can be considered as duplicates highlighting the reproducibility of the methodology.

Both experiments 4 and 5 (Table 3) have yields of magnesium in the final product of approximately 100%, indicating that practically all the magnesium added to the reaction was incorporated into the silicate structure forming amorphous magnesium silicate, which is evidenced with the $R_{m,\ actual}$ obtained in run 5, since it coincides with the $R_{m,\ theoretical}$. As the pH increases, the ionization of the silanol groups becomes greater [22]. The environment is more basic using Na_2SiO_3 with a lower SiO_2:Na_2O ratio (r). This means that using Na_2SiO_3 with r ∼ 2 silica particles with high negative charges are produced, attracting more of Mg^{2+} and increasing the yield of magnesium up to 100%. However, the product with $R_{m,\ theoretical} = 3.4$ (experiment number 4) has a $R_{m,\ actual} = 2.8$; that is, in this case there was an excess of Na_2SiO_3 that remained dissolved in the reaction bed.

As previously mentioned, Na_2SiO_3 with a lower ratio r (SiO_2:Na_2O) is characterized by mainly containing more monomers and smaller molecular groups than those with a higher ratio. This means that they have a greater number of silicate chains of shorter length. This fact causes a higher number of reaction nuclei to be present in the reaction medium, provoking all the magnesium to react and be incorporated into the structure of Na_2SiO_3. However, as noted, at high SiO_2:MgO ratios the excess of Na_2SiO_3 can act as a binding agent for the formed magnesium silicate particles, causing the BET specific surface area to decrease considerably as can be seen in Table 3. In addition to this, the decrease of the BET specific surface area in the experiment 4 may be related to the Mg incorporated in the silica network, with the result that its presence can obstruct it. Consequently, when a smaller amount of Mg^{2+} is used,

Table 4
Properties of the commercial materials and the amorphous magnesium silicates prepared (samples 6 to 9) in the industrial pilot plant at 70 °C. Samples .01, .02 and 0.03 correspond to maturation times of 0, 1 and 3 h, respectively.

SAMPLE	$R_{m,\ theoretical}$ (SiO_2:MgO)	r (SiO_2:Na_2O)	BET area (m^2/g)	$R_{m,\ real}$ (SiO_2:MgO)	Mg Yield (%)	Humidity (%)	pH	Conductivity (mS/cm)	d_{50} (μm)
6.01	3.4	3.35	605	3.9	87	5.5	10.2	0.91	72
6.02	3.4	3.35	587	-	-	-	-	-	-
6.03	3.4	3.35	650	3.9	86	3.4	10.1	0.82	125
7.01	2.4	3.35	525	-	-	-	-	-	-
7.02	2.4	3.35	566	3.7	66	7.8	8.2	2.24	95
7.03	2.4	3.35	448	3.5	67	5.5	7.8	4.25	62
8.01	3.4	2	-	-	-	-	-	-	-
8.02	3.4	2	153	3.1	97	6.4	12.1	3.04	120
8.03	3.4	2	135	3.1	95	6.1	12.1	3.45	121
9.01	2.4	2	-	-	-	-	-	-	-
9.02	2.4	2	440	2.6	100	8.2	11	0.92	16
9.03	2.4	2	453	2.6	100	7.1	11	0.82	15
Florisil®	-	-	227	4.3	-	0.8	9.6	3.5	251
Magnesia 430®	-	-	470	1.7	-	12.1	10.2	0.47	14

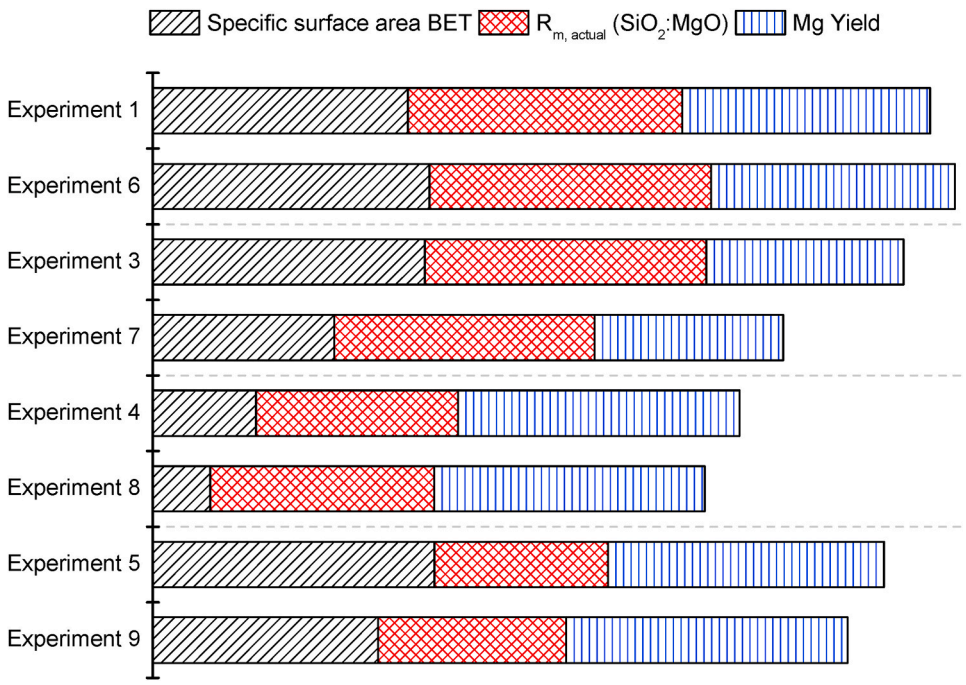

Fig. 2. Comparison between the properties of magnesium silicates obtained at laboratory and pilot plant scales. Experiments 1, 3, 4 and 5 (laboratory scale) are comparable with experiments 6, 7, 8 and 9 (industrial pilot plant), respectively.

the silica network can grow easily, leading to larger amorphous magnesium silicate particles with a lower BET specific surface area.

The amorphousness of all the materials synthesized at laboratory scale is evidenced by their corresponding XRD patterns, shown in Fig. S1.

3.2. Industrial pilot plant experiments

A series of experimental conditions previously applied in the laboratory were selected to scale up from 800 g to 700 kg of wet product obtained, i.e. by almost three orders of magnitude. These are the experiments number 1, 3, 4 and 5.

In addition to being compared with their respective experiments carried out at laboratory scale, the products obtained in the industrial pilot plant were compared with two commercial materials containing magnesium silicate. These are: Florisil® (supplier: Sigma-Aldrich), widely used as an adsorbent in chromatography due to its high selectivity [23], and Magnesia 430® (supplier: Magnesia GmbH), used in the pharmaceutical and food industries [24].

Table 4 shows the results obtained from the characterization of magnesium silicates produced in the industrial pilot plant, as well as those corresponding to the two commercial samples. The amorphousness of all these materials is evidenced by their XRD patterns, shown in Fig. S2.

First, the results obtained from the experiments carried out using the Na_2SiO_3 with a molar ratio r (SiO_2:Na_2O) $\sim$ 3.35 will be analyzed. The magnesium silicate corresponding to the experiment 6 has a BET specific surface area of ca. 600 m^2/g, approximately for the three samples 6.01, 6.02 and 6.03. A $R_{m,\ actual} = 3.9$, higher than $R_{m,\ theoretical}$ (whose value is 3.4) was obtained together with a magnesium yield close to 90%. These values are similar to those obtained in run 1 (its analogue at laboratory scale, see Table 2); as well as at laboratory scale, the product obtained did not contain all the MgO incorporated into the process as a reactant, a part of it remained in solution as Mg^{2+} ions. In addition, the samples obtained have a humidity of less than 6% with pH and conductivity values in solution of around 10 and 0.9 mS/cm, respectively. A high pH relates to a high amount of unreacted sodium silicate, while a high value of conductivity means that the water washing carried out might not be efficient enough. Furthermore, the particles have a d_{50} of around 100 μm.

The magnesium silicate corresponding to sample 7 in Table 4 has a BET specific surface area of around 500 m^2/g, with a $R_{m,\ actual}$ of ca. 3.5, higher than $R_{m,\ theoretical}$ (whose value is 2.4), and a magnesium yield close to 70%. These values are coincident with those obtained in test 3 (its analogue at laboratory scale, see Table 2). In the same way that happened at laboratory scale, a part of the magnesium introduced as a reactant remained in solution in the bed reactor. Besides, the samples obtained have a humidity of less than 8% with a pH and conductivity in solution of around 8 and less than ca. 4 mS/cm, respectively. In addition, the particles obtained are characterized by a d_{50} of ca. 90 μm. In this experiment, it is noted that sample 7.03 has a BET specific surface area smaller than those of the rest of samples; in fact, the conductivity is very high (4.25 mS/cm), which would indicate an insufficient washing of the salts, causing a lower value of BET specific surface area.

Next, the results obtained from the experiments carried out using the Na_2SiO_3 with a ratio r (SiO_2:Na_2O) ca. 2 will be analyzed. The magnesium silicate corresponding to the experiment 8 In Table 4 has a BET specific surface area of around 150 m^2/g, with a $R_{m,\ actual} = 3.1$, less than $R_{m,\ theoretical}$ (whose value is 3.4), and a magnesium yield close to 100%. In this case, as well as at laboratory scale, there was an excess of Na_2SiO_3. Moreover, the samples obtained have a humidity of less than 6.5%, with pH and conductivity in solution values of around 12 and 3 mS/cm, respectively, and the generated particles have a $d_{50} = 120$ μm.

In experiment 9, the magnesium silicate is characterized by having a BET specific surface area of around 450 m^2/g, with a $R_{m,\ actual}$ of 2.6, which could be considered similar to $R_{m,\ theoretical}$ (2.4), and a 100% magnesium yield. In addition, it has a humidity of less than 8%, with a pH and conductivity in solution of around 11 and 0.9 mS/cm, respectively. The particles obtained have a d_{50} of 15 μm.

Comparing these last two experiments, it can be seen how the particles of run 8 have a d_{50} considerably higher (ca. 120 μm) than those of experiment 9 (ca. 15 μm). This fact may be because the excess of Na_2SiO_3 in the reaction bed of test 8 acted as a binder of the magnesium silicate particles that were generated, so that their size was increased

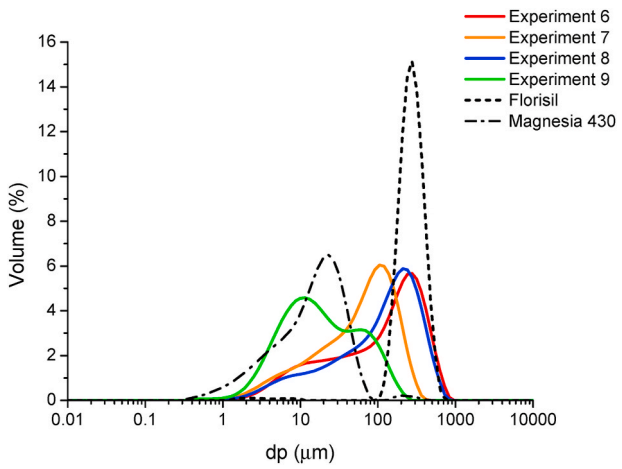

Fig. 3. Particle size distribution obtained by LD of the experiments carried out in the pilot plant and the commercial samples.

while their corresponding BET specific area values decreased. In addition, this excess of Na_2SiO_3 is evidenced by the pH and the conductivity in solution of the product obtained, since it gives higher basicity and conductivity.

The comparison between the normalized properties of BET specific surface area, $R_{m,\ actual}$ and Mg yield of the experiments carried out at laboratory scale and their similar ones in the industrial pilot plant is shown in Fig. 2, in which the high scalability of these materials is evidenced.

Fig. 3 shows the particle size distributions of the experiments carried out in the pilot plant and of the commercial samples analyzed. It is observed that the particle size distributions of the experiments performed with Na_2SiO_3 with a SiO_2:Na_2O ratio r of ca. 3.35 (experiments 6 and 7) are similar and both have a main population around 300 μm (experiment 6) and 100 μm (experiment 7) and a tail of fines. Regarding the experiments carried out with Na_2SiO_3 with a SiO_2: Na_2O ratio of ca. 2 (experiments 8 and 9) it should be mentioned that the particle size distribution of test 8 is comparable to those of the previously analyzed experiments; however, the particle size distribution of experiment 9 has two main populations, one around 10 μm and another at 65 μm. This difference between tests 8 and 9 is due to the excess of Na_2SiO_3, which makes the particles larger in the experiment 8 with the highest amount of silicate in the precipitation reaction. The particle size distributions in Fig. 3 agree with the images obtained by SEM and TEM, presented in Fig. 4. In all the cases, the images suggest a high aggregation tendency upon drying. The particle size distributions of the experiments carried out at laboratory scale are shown in Fig. S3. As it can be observed, the samples synthesized at laboratory scale have aggregation sizes higher than those obtained in the industrial pilot plant. This can be due to the different drying and grinding procedures carried out at both the laboratory and industrial scales.

The nitrogen adsorption/desorption isotherms of the amorphous

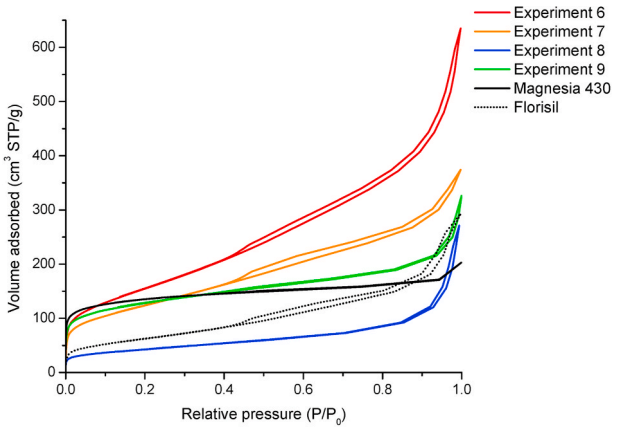

Fig. 5. Nitrogen adsorption/desorption isotherms of the amorphous magnesium silicates obtained in the industrial pilot plant and the commercial samples.

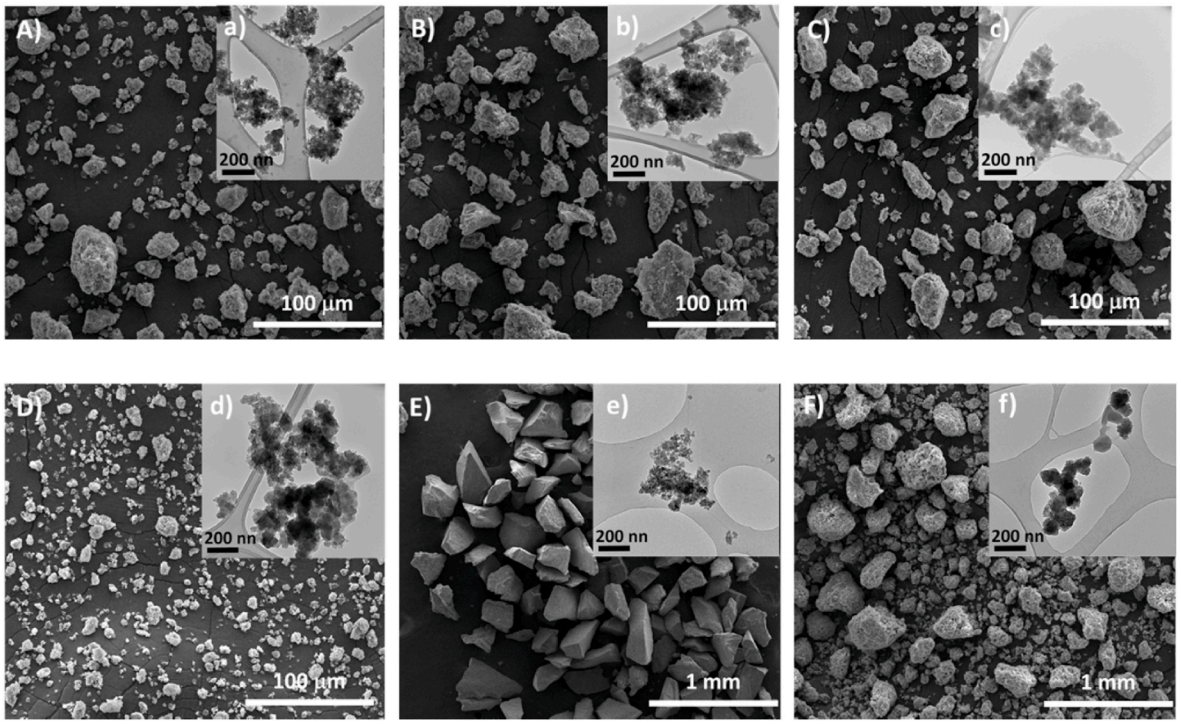

Fig. 4. SEM images: A) experiment 6, B) experiment 7, C) experiment 8, D) experiment 9, E) Florisil®, F) Magnesia 430®, with insets showing TEM images of the same samples (a–f).

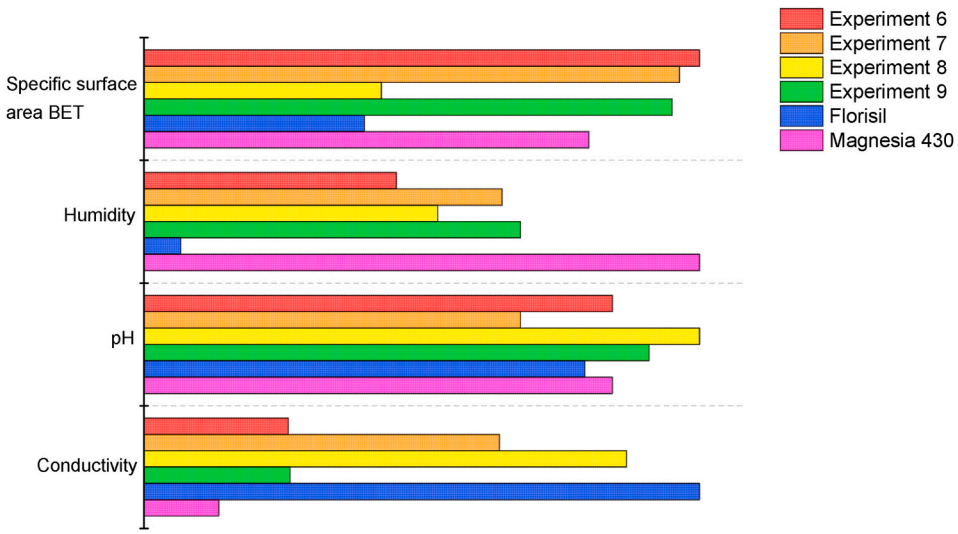

Fig. 6. Comparison between the properties of magnesium silicates obtained in pilot plant and the commercial samples.

magnesium silicates carried out in the industrial pilot plant, as well as those of the commercial samples analyzed, are presented in Fig. 5. It can be seen that experiments 6 and 7 and Florisil® exhibit a type IV isotherm with an evident type H3 hysteresis loop, consistent with the presence of mesoporous in the materials. Loops of this type are normally given by non-rigid aggregates of plate-like particles [25]. It should be noted that experiments 6 and 7 were carried out with a SiO_2:Na_2O ratio r of ca.3. 35. Furthermore, experiments 8 and 9, which were performed with a SiO_2:Na_2O ratio r of ca. 2.0, show a type IV isotherm with a type H1 hysteresis loop. This type of loop is found in materials which exhibit a narrow range of uniform mesoporosity [25]. In type IV isotherms the amount of adsorbed nitrogen slightly increased until the relative pressure of 0.8 was obtained. At higher values of relative pressure an abrupt increase was noted in the amount of adsorbed nitrogen. That course of adsorption isotherms agrees with the fact that these products are mesoporous sorbents (where the amount of adsorbed nitrogen practically did not increase until the relative pressure reached the value of 0.8) [10, 15], which is evidenced by their mean pore diameter, obtained by the BJH method, shown in Table S2 (in the 5.2–14.2 nm range). Finally, it is noted that the isotherm of the commercial sample Magnesia 430® has no hysteresis loop and is a mixture of type I and type II isotherms, resulting from microporous and an external surface area, in comparison with the other samples that mainly have an external surface. The external surface area and micropore area, obtained by the t-plot method, of all these samples are shown in Table S2. In addition, the BJH-pore size distributions are presented in Fig. S4, where it can be observed that the pore sizes of all the samples are much less than the particle sizes observed by TEM (see Fig. 4 insets). These observations suggest a structural porosity of the particles and discards pores exclusively between aggregate particles.

From another point of view, these amorphous magnesium silicates have properties that are within the range of the commercial products analyzed in this work (see Fig. 6). On the one hand, Florisil® is characterized by a BET specific surface area of 227 m^2/g, with $R_{m,\ actual}$ = 4.3, humidity of 0.8% and pH and conductivity in solution values of 9.6 and 3.5 mS/cm, respectively. In addition, it has a d_{50} of 251 μm. On the other, Magnesia 430® has a BET specific surface area of 470 m^2/g, a $R_{m,\ actual}$ = of 1.7, humidity of 12.1% and a pH and conductivity in solution of 10.2 and 0.5 mS/cm, respectively; in addition to a d_{50} of 14 μm.

Fig. 6 shows the normalized properties of BET specific surface area, humidity, pH and conductivity of the experiments carried out in the industrial pilot plant with the results of the commercial products. It is worth mentioning that the d_{50} is not represented because it is strongly related to the type of equipment used for drying the particles and some samples would not be comparable with others. In any event, it can be highlighted that the BET specific surface area values of the samples obtained here are superior to those of the commercialized magnesium silicate products, what might suggest a good performance for our materials in adsorption and ion exchange applications.

4. Conclusions

In this study, amorphous magnesium silicates with different SiO_2: MgO molar ratios have been synthesized at both laboratory and pilot plan scales, finding promising results in the experiments carried out in the industrial pilot plant. After the results obtained, the following conclusions can be drawn:

- The maturation time did not influence the final properties of the amorphous magnesium silicates obtained. This can be due to the fast precipitation process at the conditions studied.
- It was observed, both in laboratory experiments and those carried out in the industrial pilot plant, that the SiO_2:Na_2O ratio (r) of the Na_2SiO_3 used as a reagent is a key parameter in the synthesis of amorphous magnesium silicates. With a high ratio (r $\sim$ 3.35), Na_2SiO_3 was not enough depolymerized so that the magnesium yield on the final product was less than 100%. On the other hand, with a low ratio (r $\sim$ 2), Na_2SiO_3 was sufficiently depolymerized so that all the magnesium incorporated as a reagent entered into the solid structure to form magnesium silicate. However, it is necessary to look for a compromise, since with a low r of the Na_2SiO_3, but a high SiO_2: MgO molar ratio (as it is 3.4) in magnesium silicate, a certain amount of Na_2SiO_3 reaction centers remained unreacted.
- Different SiO_2:Na_2O ratios of Na_2SiO_3 gave rise to different nitrogen adsorption/desorption isotherms. Experiments performed with a SiO_2:Na_2O ratio r of ca. 2.0 showed a type IV isotherm with a type H1 hysteresis loop, resulting from a narrow range of uniform mesoporous. While the experiments with a SiO_2:Na_2O ratio r of ca. 3.35 showed a type IV isotherm with a type H3 hysteresis loop, consistent with the presence of mesoporous in the materials and non-rigid aggregates of plate-like particles.
- The synthesized amorphous magnesium silicates are characterized by having a good scalability (with an increase in scale with respect to laboratory experiments of approximately 10^3), because similar properties (BET specific surface area, SiO_2: MgO molar ratio and magnesium yield on the products) were obtained at laboratory scale and industrial pilot plant scale.

- Amorphous magnesium silicates have been synthesized in an industrial pilot plant with promising properties (in terms of BET specific surface area, humidity, pH and conductivity in solution and particle size distribution), since these are within the range of properties corresponding to typical commercial magnesium silicates, with higher values for some parameters such as the BET specific surface area.

CRediT authorship contribution statement

Yolanda Aysa-Martínez: Laboratoy work, Methodology, Formal analysis, Writing – original draft, Writing – review & editing. **Silvia Anoro-López:** Laboratory work, Methodology, Formal analysis. **Miguel Cano:** Conceptualization, Methodology, Supervision, Writing – original draft, Writing – review & editing. **Daniel Julve:** Conceptualization, Methodology, Supervision, Writing – original draft, Writing – review & editing. **Jorge Pérez:** Conceptualization, Methodology, Supervision, Project administration, Funding acquisition, Writing – original draft, Writing – review & editing. **Joaquín Coronas:** Conceptualization, Methodology, Supervision, Project administration, Funding acquisition, Writing – original draft, Writing – review & editing.

Declaration of competing interest

The authors declare that they have no known competing financial interests or personal relationships that could have appeared to influence the work reported in this paper.

Acknowledgements

Y. Aysa-Martínez acknowledges Industrias Químicas del Ebro, S.A. for the predoctoral funding.

Appendix A. Supplementary data

Supplementary data to this article can be found online at https://doi.org/10.1016/j.micromeso.2021.110946.

References

[1] A.E. Ringwood, A. Major, High-pressure reconnaissance investigations in the system Mg2SiO4-MgO-H2O, Earth Planet Sci. Lett. 2 (1967) 130–133, https://doi.org/10.1016/0012-821X(67)90114-8.
[2] L. Liu, Effects of H20 on the phase behaviour of the forsterite–enstatite system at high pressures and temperatures and implications for the Earth, Phys. Ofthe Earth Planet. Inter. 49 (1987) 142–167, https://doi.org/10.1016/0031-9201(87)90138-5.
[3] M. Kanzaki, Stability of hydrous magnesium silicates in the mantle transition zone, Phys. Earth Planet. In. 66 (1991) 307–312, https://doi.org/10.1016/0031-9201(91)90085-V.
[4] E. Ohtani, H. Mizobata, Y. Kudoh, T. Nagase, A new hydrous silicate, a water reservoir, in the upper part of the lower mantle, Geophys. Res. Lett. 24 (1997) 1047–1050, https://doi.org/10.1029/97GL00874.
[5] T. Gasparik, The role of volatiles in the transition zone, J. Geophys. Res. 98 (1993) 4287–4299, https://doi.org/10.1029/92JB02530.
[6] D.J. Frost, Stability of hydrous magnesium silicates in the mantle transition zone, Geochemical Soc 6 (1999).
[7] J.T. Kloprogge, S. Komarneni, J.E. Amonette, Synthesis of smectite clay minerals: a critical review, Clay Clay Miner. 47 (1999) 529–554, https://doi.org/10.1346/CCMN.1999.0470501.
[8] A.G. Kalampounias, N. Bouropoulos, K. Katerinopoulou, S.N. Yannopoulos, Textural and structural studies of sol-gel derived CaO- and MgO silica glasses, J. Non-Cryst. Solids 354 (2008) 749–754, https://doi.org/10.1016/j.jnoncrysol.2007.07.076.
[9] A. Krysztafkiewicz, L.K. Lipska, F. Ciesielczyk, T. Jesionowski, Amorphous magnesium silicate - synthesis, physicochemical properties and surface morphology, Adv. Powder Technol. 15 (2004) 549–565, https://doi.org/10.1163/1568552042000183.
[10] F. Ciesielczyk, A. Krysztafkiewicz, T. Jesionowski, Physicochemical studies on precipitated magnesium silicates, J. Mater. Sci. 42 (2007) 3831–3840, https://doi.org/10.1007/s10853-006-0464-2.
[11] J. Liao, M. Senna, Enhanced dehydration and amorphization of Mg(OH)2 in the presence of ultrafine SiO2 under mechanochemical conditions, Thermochim. Acta 210 (1992) 89–102, https://doi.org/10.1016/0040-6031(92)80280-A.
[12] F. Ciesielczyk, A. Krysztafkiewicz, T. Jesionowski, Influence of precipitation parameters on physicochemical properties of magnesium silicates, Physicochem. Probl. Miner. Process. 38 (2004) 197–205.
[13] B. Ghods, M. Rezaei, F. Meshkani, Synthesis of nanostructured magnesium silicate with high surface area and mesoporous structure, Ceram. Int. 42 (2016) 6883–6890, https://doi.org/10.1016/j.ceramint.2016.01.073.
[14] F. Ciesielczyk, A. Krysztafkiewicz, K. Bula, T. Jesionowski, Evaluation of synthetic magnesium silicate as a new polymer filler, Compos. Interfac. 17 (2010) 481–494, https://doi.org/10.1163/092764410X513314.
[15] B. Adams, E. Holmes, Adsorptive properties of synthetic resins, J. Soc. Chem. 54 (1935) 1–6.
[16] F. Ciesielczyk, A. Krysztafkiewicz, T. Jesionowski, Magnesium silicates - adsorbents of organic compounds, Appl. Surf. Sci. 253 (2007) 8435–8442, https://doi.org/10.1016/j.apsusc.2007.04.016.
[17] O.O. Taspinar, S. Ozgul-Yucel, Lipid adsorption capacities of magnesium silicate and activated carbon prepared from the same rice hull, Eur. J. Lipid Sci. Technol. 110 (2008) 742–746, https://doi.org/10.1002/ejlt.200700313.
[18] I. Rashid, N.H. Daraghmeh, M.M. Al Omari, B.Z. Chowdhry, S.A. Leharne, H. A. Hodali, A.A. Badwan, Profiles of Drug Substances, Excipients and Related Methodology, vol. 36, Academic Press, 2011.
[19] K. Yanagisawa, K. Masaki, K. Someno, Method for Producing Rubber-Filler Master Batch, US20090018238A1, 2009.
[20] A. Takashi, A. Ryuichi, S. Mamoru, M. Naoya, M. Megumi, S. Masako, Recording Paper and Ink Jet Recording Method by Use Thereof, US4758461, 1988.
[21] J. Nordström, A. Sundblom, G. Vestergaard, J. Skov, A. Palmqvist, A. Matic, Silica/alkali ratio dependence of the microscopic structure of sodium silicate solutions, J. Colloid Interface Sci. 397 (2013) 9–17, https://doi.org/10.1016/j.jcis.2013.01.048.
[22] R.K. Iler, The Chemistry of Silica: Solubility, Polimerization, Colloids and Surface Properties, and Biochemistry, Wiley-Interscience, New York, 1979.
[23] M. Waksmundzka-Hajnos, Properties of Florisil and its use in chromatography, J. Anal. Chem. 301 (1998).
[24] Magnesia (n.d.), https://www.magnesia.de/en/products/product-overview.html. (Accessed 5 May 2019). accessed.
[25] M. Thommes, K. Kaneko, A.V. Neimark, J.P. Olivier, F. Rodriguez-Reinoso, J. Rouquerol, K.S.W. Sing, Physisorption of gases, with special reference to the evaluation of surface area and pore size distribution (IUPAC Technical Report), Pure Appl. Chem. 87 (2015) 1051–1069, https://doi.org/10.1515/pac-2014-1117.